Deep Learning Using High-Resolution Images of Forearm Predicts Fracture

Running head: Fracture Prediction using Deep Learning

Roland Chapurlat[1]
Serge Ferrari[2]
Xiaoxu Li[3]
Yu Peng[3]
Min Xu[4]
Min Bui[5]
Elisabeth Sornay-Rendu[1]
Eric lespessailles[6]
Emmanuel Biver[2]
Ego Seeman[7]

[1]INSERM UMR 1033, Université Claude Bernard-Lyon1, Hospices Civils de Lyon, Lyon, France
[2]University of Geneva, Geneva, Switzerland
[3]CurvebeamAI, Melbourne
[4]University of Technology Sydney
[5]Centre for Epidemiology and Biostatistics, School of Population and Global Health, University of Melbourne, Melbourne, Australia
[6]IPROS, CHR d'Orléans
[7]Depts Endocrinology and Medicine, Austin Health, University of Melbourne[1]

Correspondence: Roland Chapurlat

Key Points

Question Can a deep learning model (DL)° based on high resolution images of the distal forearm predict fragility fractures?

Findings In the setting of 3 pooled population-based cohorts, the DL model predicted fractures substantially better than areal bone mineral density and FRAX, especially in women ≥65 years.

Meaning Our DL model may become an easy to use way to identify postmenopausal women at risk for fracture to improve fracture prevention.

Abstract

Importance Fragility fractures are a public health problem. Over 70% of women having fractures have osteopenia or normal BMD, but they remain unidentified and untreated because the definition of 'osteoporosis', a bone mineral density (BMD) T-Score ≤ -2.5SD, is often used to signal bone fragility.

Objective As deep learning facilitates investigation of bone's multi-level hierarchical structure and soft tissue, we tested whether this approach might better identify women at risk of fracture before fracture.

Design We pooled data from three French and Swiss prospective population-based cohorts (OFELY, QUALYOR, GERICO) that collected clinical risk factors for fracture, areal BMD and distal radius measurements with high resolution peripheral quantitative tomography (HRpQCT). Using only three-dimensional images of the distal radius, ulna and soft tissue acquired by HRpQCT, an algorithm, a Structural Fragility Score-Artificial Intelligence (SFS-

AI), was trained to distinguish 277 women having fractures from 1401 remaining fracture-free during 5 years and then was tested in a validation cohort of 422 women.

Setting European postmenopausal women

Participants We have studied postmenopausal women considered as representative of the general population, who were followed for a median 9.4 years in OFELY, 5.4 years in QUALYOR and 5.7 years in GERICO.

Main outcome and measure All types of incident fragility fractures

Results We used data from 2666 postmenopausal women, with age range of 42-94. In women ≥ 65 years having 'All Fragility Fractures' or 'Major Fragility Fractures', SFS-AI generated an AUC of 66-70%, sensitivities of 60-68% and specificity of 71%. Sensitivities were greater than achieved by the fracture risk assessment (FRAX) with BMD or BMD (6.7-26.7%) with lower specificities than these diagnostics (~95%).

Conclusion and relevance The SFS-AI is a holistic surrogate of fracture risk that pre-emptively identifies most women needing prompt treatment to avert a first fracture.

Key words: Artificial Intelligence, Bone Structure, Bone Fragility, Deep Learning, Fractures

Introduction

Fragility fractures are a public health problem because fractures impose high morbidity, mortality and cost to the community.[1] To identify women with fragile bones before fracture, a W.H.O group designated women as having 'osteoporosis' if femoral neck bone mineral density (BMD) T-Score was ≤ -2.5 standardized deviations (SD) below the premenopausal mean.[2] Epidemiological studies confirmed that fracture risk increases as BMD decreases, but the frequency distribution around the age-related decline in mean BMD remains normal.

Because of this normal frequency distribution, most postmenopausal women in the community have osteopenia (T-score -2.5 to -1.0 SD) or normal BMD (T-score > -1.0 SD). These women form the source of 75% of all fragility in the community, only 25% arise among the smaller subset of women in the community with osteoporosis as defined by BMD.[3-9] The women with osteopenia or normal BMD having fragility fractures remain unidentified and untreated using the definition of osteoporosis, a BMD T-Score ≤ - 2.5 SD, to signal bone fragility. Treatment is not offered, even in the presence of a prevalent or incident fracture, because the absence of osteoporosis is incorrectly interpreted as being evidence of absence of bone fragility.[10]

Osteoporosis and bone fragility are used interchangeably even though they are not synonymous terms.[11-13] Absence of osteoporosis does not exclude bone fragility. Bone fragility is not binary, present in women with osteoporosis (T-Score ≤ -2.5 SD) and absent in women without osteoporosis (T-Score > -2.5 SD). Even when bone loss only reduces BMD into the low normal or osteopenia range, the bone is unlikely to be 'normal'. Bone mass is reduced relative to premenopausal women and many qualities of bone responsible for its strength may be compromised.[14-18]

For example, advancing age deteriorates the composition of the mineralized matrix.[19,20] Bone loss disrupts the spatial configuration of bone's three-dimensional architecture.[15,21] These changes produce a non-linear increase in bone fragility, disproportionate to both the bone loss causing the deterioration and the reduction in BMD.[20,22] Resistance to bending is a 7th power function of bone's cortical porosity and a 3rd power function of its trabecular density.[22]

Consequently, even modest disruption of the spatial configuration of bone at nano-, and micro-levels of resolution compromise bone strength independent of BMD. In addition, soft tissue changes like loss of muscle mass (sarcopenia) impair mobility and balance predisposing to falls, fractures and mortality.[23] Thus, reducing the population burden of fractures requires a diagnostic that complements BMD by identifying women at risk of fracture due to bone fragility caused by compromised bone morphology not captured by BMD $\leq$ - 2.5 SD, by an increased risk of falls due to deteriorated soft tissues such as muscle mass, or both. Non-invasive evaluation of bone microarchitecture improves fracture prediction compared with FRAX plus BMD or BMD alone.[8,9]

A promising area of innovation in the promotion of human health is the use of Artificial Intelligence (AI). Application of Deep Learning to medical imaging[24] facilitates the investigation of bone's multilayered qualities and has been reported to identify patients with prevalent fractures or osteoporosis in cross sectional studies.[25-27] However, no prospective studies have applied deep learning using only the high resolution 3-dimensional images of bone and soft tissue to determine whether an algorithm, a Structural Fragility Score derived by Artificial Intelligence (SFS-AI), might capture deteriorated bone qualities and soft tissue. If so, this holistic surrogate of fracture risk is likely to serve as a diagnostic that pre-emptively

identifies women at risk of a first or subsequent fracture needing prompt treatment and would do so better than the fracture risk assessment (FRAX) score with BMD or BMD alone.

Methods

Participants We studied (i) 568 postmenopausal women, median age 68.2 years, range 42-94 of Os des FEmmes de LYon, OFELY, France followed for a median [interquartile range] of 9.4 [1.0] years,[9,28,29] (ii) 1427 women of the Qualité Osseuse Lyon Orléans, QUALYOR cohort (1042 recruited in Lyon, 497 in Orléans), median age 65.9 (range 50-87) years followed for 5 years[30] and (iii) 671 women of the Geneva Retirees Cohort, GERICO, in Switzerland median age 65 (range 63-68) years followed 5.7 years (range 2-8).[31] The studies were approved by the institutional review boards. Participants provided informed consent. Fractures (excluding head, toes and fingers) were confirmed using radiographs.

Bone microarchitecture, bone densitometry, FRAX with BMD HRpQCT (voxel size of 82 μm^3) was used to scan the non-dominant forearm (Scanco Medical AG, Switzerland).[32] Radiation exposure was ~3 microsievert. Quality control was monitored by daily scans of hydroxyapatite rods (QRM, Moehrendorf, Germany). Femoral neck BMD was quantified using Hologic DXA scanners in the French cohorts and Hologic QDR Discovery in the Swiss cohort. T-scores were calculated using NHANES III. FRAX with femoral neck BMD provides a 10-year risk for Major Fragility Fractures (proximal humerus, wrist, distal forearm, clinical spine, or hip).[33]

Deep Learning network To avoid bias towards any one of the three cohorts, we combined the three cohorts and then we randomly divided the combined data set into a training and testing data set. No training data was used as testing data. **Figure S2** shows participants were randomly allocated to five groups, four used for training (n=1678), the fifth used for testing (n = 422). Scores were calculated for each testing group with the median forming the SFS-AI (see Supplement **Figure S2**). Deep learning was applied to images of the

distal radius and ulna and the surrounding soft tissue acquired using HR-pQCT (see Supplement).[34-37] Training the algorithm to identify women sustaining fractures faced two challenges: (i) extraction of features within the three-dimensional image captured by a matrix of 110*1560*1560 voxels conferring fracture risk and (ii) limited data for training predisposing to model over-fitting. We used the DenseNet121 as the feature extraction network (**Figure S1**). Features conferring fracture risk were learnt collectively by densely connected layers in the neural network. The input to the feature extraction network was the 110 slices acquired by the HR-pQCT at the distal radius (including the ulna and surrounding soft tissues). The output from the feature extraction network is a feature vector of 256 numbers.

To achieve robust feature extraction, a multi-task learning strategy was used to overcome model overfitting. To provide pictorial representation of the fracture risk prediction, extracted features were displayed as a heat map overlaid upon a 2D projection of the images. Red reflects greater relevance of the region's bone or soft tissue to fracture prediction.

Statistical Analyses Analyses were conducted using data in women of any age and those 65 years and over. Follow-up was to fracture or freedom from fracture for five years since HR-pQCT scanning. SFS-AI, FRAX with BMD and BMD were not normally distributed and so are presented as median and interquartile range (IQR). Values are adjusted for age and cohort because of cohort differences in age and follow-up duration. (**Tables S1** and **S2.)** Comparison of the diagnostics in women having fractures and those remaining fracture-free was carried out using analysis of covariance adjusted for age and cohort and estimated by robust regression. (**Table 1.**)

The performance of SFS-AI as a continuous trait was assessed using the area under the curve (AUC) and was estimated using a parametric probit model[38] and logistic regression to derive Odds Ratios (ORs) for fracture. Both analyses are presented unadjusted and adjusted for age and cohort effect. The sensitivity and specificity of SFS-AI as a binary trait used a threshold of 0.5. (Addressed in **Table 2.**)

We also assessed the performance of FRAX with BMD and BMD as continuous traits using ROC analysis and computed sensitivity and specificity using thresholds of 20% for FRAX with BMD and – 2.5 SD for BMD denoting high fracture risk. Logistic regression was then used to assess any association of these diagnostics with fracture, separately and combined, for women of any age and women aged 65 years and over. (Addressed in **Figure 1 and Table S3.**)

Linear regression was used to assess the association of SFS-AI with age, separately for women with fractures and women remaining fracture-free. (Addressed in **Figure 2.**) Age, cortical porosity, trabecular density, FRAX with BMD and BMD were used in linear regression to compute an overall R-squared and to determine the proportion of variance in SFS-AI explained by these independent variables. The percentage contribution of each trait to the overall R-squared was computed using the Shapley method.[39] (Addressed in **Table S5** and **Figure 3.**)

Results

Table 1 shows SFS-AI was higher in women having 'All' or 'Major Fragility Fractures' than women remaining fracture-free (both $p < 0.001$). Neither FRAX with BMD nor BMD alone differed in women having fractures versus those remaining fracture-free ($p > 0.15$).

SFS-AI pre-emptively identifies women at risk of 'All' and 'Major Fragility Fractures'

Table 2 shows that in the testing cohort of 422 women of any age and the 236 women ≥ 65 years of age, the SFS-AI as a continuous trait generated AUCs of 73-74% for 'All Fragility Fractures' and 'Major Fragility fractures' with adjusted ORs ranging from 2.53 to 2.67 per standard deviation. The SFS-AI as a categorical trait (using a threshold of 0.5), had sensitivities ranging from 58.1% to 74.0% and specificities ranging from 71.0% to 77.3% (all significant, $p < 0.001$ for OR and AUC.

Comparing SFS-AI with FRAX with BMD and BMD

Women of any age Comparisons of the diagnostics was confined to participants having all three measurements. **Figure 1** shows the diagnostics as continuous traits. For 'All Fragility Fractures' and 'Major Fragility Fractures', the AUCs for SFS-AI were 72% and 69% respectively ($p < 0.05$). **Table S3** shows unadjusted and adjusted SFS-AI predicted women having either category of fractures (ORs ranged from 2.07 to 2.41, all $p < 0.001$). Neither of the other two diagnostics predicted either category of fracture. **Figure 1** also shows the diagnostics as categorical traits. For SFS-AI, sensitivities were 59.3% and 50.0% for detecting women having 'All Fragility Fractures' or 'Major Fragility Fractures' respectively, values that were significantly greater than sensitivities of FRAX with BMD or BMD (which

ranged 4.2 to 16.7%). Specificities of SFS-AI were 77.1%, significantly lower than specificities of the other two diagnostics (which ranged 94.6 to 96.6%).

Women aged ≥ 65 years Supplementary **Figure S3** shows the performance of the diagnostics as continuous traits. For 'All Fragility Fractures' and 'Major Fragility Fractures', the AUCs for SFS-AI were 70% and 66% respectively. **Table S4** shows unadjusted and adjusted SFS-AI predicted both categories of fractures (OR 1.68 to 2.15, all $p < 0.05$). Neither of the other two diagnostics predicted either category of fracture. **Figure S3** also shows the performance of the diagnostics as categorical traits. For SFS-AI, sensitivities were 67.6% and 60.0% for detecting women having 'All Fragility Fractures' or 'Major Fragility Fractures' respectively, values significantly greater than the sensitivities of FRAX with BMD or BMD (ranging 6.67 to 26.7%). Specificities of SFS-AI were 70.7%, significantly lower than specificity of 94.6% for the other two diagnostics.

The morphological basis of the SFS-AI **Figure 2** shows that SFS-AI increased across age in women having fragility fractures and in women remaining fracture-free. Red regions of the heat map overlying bone and soft tissue identify regions of high relevance to risk of incident fractures compared to the blue regions. **Figure 3** shows that SFS-AI correlated with microarchitecture; directly with cortical porosity and FRAX with BMD, and negatively with trabecular density and BMD. **Figure 3** and Supplementary **Table S5** show that 46% of the variance in SFS-AI was explained by variance in age ($p = 0.002$), cortical porosity and trabecular density (both $p < 0.001$) but not with BMD or FRAX with BMD; 54% of the variance remained unexplained.

Discussion

A deep learning algorithm was trained to identify women having fragility fractures using only the high-resolution three-dimensional images of bone and soft tissue. No other information was used. When training no longer improved predictive strength, the algorithm was tested in a cohort without knowledge of their fracture status during the ensuing 5 years. This algorithm served as a surrogate of fracture risk, predicting the incidence of 'All Fragility Fractures' and 'Major Fragility Fractures' and did so in women 65 years and older with a sensitivity and specificity of 60-70%, out-performing BMD and FRAX with BMD, neither of which predicted fractures.

This surrogate of fracture risk, a Structural Fragility Score derived by deep learning artificial intelligence, increased across advancing age, was higher in women having incident fractures than those remaining fracture-free, and correlated directly with cortical porosity and negatively with trabecular density. Deterioration of these two traits produces a nonlinear increase in bone fragility,[22] predicts incident fractures,[8,9] prevalent fractures[40] and predicts estimated bone strength independent of BMD.[41] Deterioration of these two traits accounted for most of the 48% explained variance in SFS-AI. BMD was not an independent predictor of SFS-AI.

Many qualities of bone not captured by BMD but not yet quantifiable non-invasively, may contribute to the 54% of the unexplained variance in this surrogate of fracture risk.[14-19] For example, heterogeneity in bone's material composition forms discontinuities, edges, that defend against fracture by increasing the energy required to initiate and propagate a crack.[42] Small changes in the degree of mineralization increase matrix stiffness but reduce its ductility (ability to absorb energy by deforming).[43] Heterogeneity in the size and number of osteons,[44]

the cement line around each osteon,[45,46] the differing orientation of mineralized collagen fibres of adjacent concentric osteonal lamellae,[47-49] the extent glycation,[50] hydration[51] and other factors[52,53] influence the mechanical properties of bone. The heat map implicated deterioration of soft tissue as well as bone. The nature of soft tissue deterioration is not known but if it is sarcopenia then the SFS-AI algorithm might capture a component of risk for falls.[23]

Most studies using machine learning are cross sectional and examine the ability to identify persons with prevalent fractures or osteoporosis (BMD T-Score ≤ - 2.5 SD).[24-27] This is the first prospective study using deep learning to derive an algorithm that identifies women having incident fractures during five years. The algorithm was developed by interrogating the three-dimensional images of bone and soft tissue, no other information was used. This Structural Fragility Score serves as a surrogate of fracture risk that is likely to assist in reducing the population burden of fragility fractures. It provides a diagnostic able to identify most women at risk of fracture and provides fast processing, easy access to risk assessment allowing prompt initiation and monitoring of preventative treatment at the community level.

High resolution peripheral quantitative computed tomography (HRpQCT) technology is no-longer confined to the research domain. Commercial devices are now CE marked and FDA cleared for multiple clinical settings. Analysis requires only the acquisition of the three-dimensional image of the distal radius, ulna and soft tissue and cloud-based computer technology provides prompt diagnosis allowing initiation or monitoring of therapy.

This study has several limitations. Further studies are needed to determine whether including factors predisposing to falls such as muscle mass and function, age, height, weight and other

366 covariates improves the performance of the diagnostic. The sample sizes were insufficient to
367 evaluate performance of the diagnostic in predicting individual types of fracture.
368
369 Advancing age is accompanied by deterioration in bone mass, its material composition,
370 architecture and muscle mass - factors contributing to fragility fractures, a public health
371 problem. High-resolution quantitative computed tomography and deep learning provide a
372 Structural Fragility Score that serves as a holistic surrogate of fracture risk. This diagnostic is
373 an accurate, safe, rapid and easily accessible tool that captures the deterioration of bone
374 qualities contributing to bone fragility independent of BMD and perhaps deterioration of
375 muscle predisposing falls. This surrogate identifies women at high risk of fracture needing
376 prompt treatment to avert fracture and may allow monitoring the success or failure of
377 treatment.
378
379
380
381
382
383
384
385
386
387
388
389
390
391

Legends for Figures for manuscript

Figure 1. Left two panels: Receiver Operator Characteristic (ROC) curves for Structural Fragility Score Artificial Intelligence (SFS-AI), Fracture Risk Assessment Score (FRAX) with bone mineral density (BMD) and BMD as a continuous trait predicting for 'All Fragility Fractures' and 'Majority Fragility Fractures' for women of any age. Area under the Curves (AUCs) with 95% Confidence Intervals (CI) were significant (*$p < 0.05$) for SFS-AI only. **Right two panels:** Sensitivity and specificity of SFS-AI, FRAX with BMD and BMD as categorical traits.

Figure 2. Left panels: Advancing age is associated with a higher Structural Fragility Score-Artificial Intelligence (SFS-AI) in women having 'All Fragility Fractures' or Major Fragility Fractures (closed circles) and in women remaining fracture-free (open circles). The images of the distal radius and ulna with the heat map illustrate regions commonly encountered in women having fractures.

Figure 3. Left panels. The Structural Fragility Score-Artificial Intelligence (SFS-AI) was associated directly with cortical porosity, FRAX with BMD and negatively with trabecular density and BMD. **Right diagram**. Of the 47% of explained variance in the SFS-AI, most was attributed to trabecular density, cortical porosity, age and the FRAX with BMD. The contribution of BMD was not significant. The remaining 53 percent remained unexplained.

Legends for Figures in supplementary material

Figure S1. Structure of the deep learning model used to predict fracture. The input is the 110 slices of a wrist scan used to acquire the three-dimensional image of the distal radius, distal

ulna and adjacent soft tissue. DenseNet121 is used as the neural network backbone. The output feature after the global average pool is a 256-dimension feature. A multi-task (age prediction, fracture prediction and non-fracture years prediction) learning strategy was used to achieve robust extraction of relevant features.

Figure S2. We studied women from OFELY (n = 568), Qualyor (n = 1427) and Gerico (n = 671). (A) There were 526, 1187 and 387 images remaining from the respective cohorts for analysis after excluding images from women remaining fracture-free followed for under 5 years and images from women having traumatic (non-fragility). (B) Women having a fragility fracture during 5 years were denoted as (+), women remaining fracture-free as (-). (C) Participants from each cohort were randomly allotted into five groups with approximately equal numbers of (+) and (-) subjects. See Methods section.

Figure S3. Left two panels. Receiver Operator Characteristic (ROC) curves for Structural Fragility Score Artificial Intelligence (SFS-AI), Fracture Risk Assessment Score (FRAX) with bone mineral density (BMD) and BMD as continuous traits predicting 'All Fragility Fractures' and 'Major Fragility Fractures' in women 65 years of age and over. Area under the Curves (AUCs) with 95% Confidence Intervals (CI) were significantly different from 0.5 (*$p < 0.05$) for SFS-AI only. **Right two panels.** Sensitivity and specificity of the SFS-AI, FRAX with BMD and BMD as categorical traits predicting women having 'All Fragility Fractures' or 'Major Fragility Fractures'.

References

1. Compston JE, McClung M, Leslie W. Osteoporosis. Lancet 2019;393: 364-76

2. Kanis JA. Assessment of fracture risk and its application to screening for postmenopausal osteoporosis: synopsis of a WHO report. WHO Study Group. Osteoporos Int. 1994;4: 368–81.

3. Siris ES, Chen YT, Abbott TA, et al. Bone mineral density thresholds for pharmacological intervention to prevent fractures. Arch Intern Med. 2004;164: 1108–12.

4. Schuit SC, van der Klift M, Weel AE, et al. Fracture incidence and association with bone mineral density in elderly men and women: the Rotterdam Study. Bone. 2004;34:195–202.

5. Pasco JA, Seeman E, Henry MJ, et al. The population burden of fractures originates in women with osteopenia, not osteoporosis. Osteoporos Int. 2006;17:1404–9.

6. Sanders KM, Nicholson GC, Watts JJ, et al. Half the burden of fragility fractures in the community occur in women without osteoporosis. When is fracture prevention cost-effective? Bone. 2006;38: 694–700.

7. Trajanoska K, Schoufour JD, de Jonge EAL et al. Fracture incidence and secular trends between 1989 and 2013 in a population-based cohort: The Rotterdam Study Bone. 2018;114:116–24.

8. Samelson EJ, Broe KE, Xu H et al. Cortical and trabecular bone microarchitecture as an independent predictor of incident fracture risk in older women and men in the Bone Microarchitecture International Consortium. Lancet Diabetes *Endocrinol.* 2019;7:34-43.

9. Chapurlat R, Bui M, Sornay-Rendu E, Seeman E et al. Deterioration of cortical and trabecular microstructure identifies women with osteopenia or normal bone mineral density at imminent and long-term risk for fragility fracture: a prospective study. J Bone Miner Res 2020; 35: 833-44.

10. Leslie WD, Seeman E, Morin SN, Lix LM, Majumdar SR. The diagnostic threshold for osteoporosis impedes fracture prevention: A registry-based cohort study. Bone 2018; 114:298-303.

11. Colon-Emeric CS, Saag KG. Osteoporotic fractures in older adults. Best Pract Res Clin Rheumatol. 2006;20(4):695–706.

12. Lyles K, Gold D, Shipp K, et al. Association of osteoporotic vertebral compression fractures with impaired functional status. Am J Med.1993;94:595–601.

13. Diamond T, Champion B, Clark W. Management of acute osteoporotic vertebral fractures: a non-randomized trial comparing percutaneous vertebroplasty with conservative therapy. Am J Med. 2003; 114:257–65.

14. Weiner S, Traub W (1992) Bone structure: from angstroms to microns. FASEB J 6:879–885

15. Seeman E, Delmas PD. Bone quality – the material and structural basis of bone strength and fragility. New Engl J Medicine. 2006;354:2250-61.

16. Muller R. Hierarchical microimaging of bone structure and function. Nature Rev. Rheumatol. 2009; 5:373-81.

17. Ural A, Vashishth D. Hierarchical perspective of bone toughness-from molecules to fracture. Int Mater Rev 2014; 59:245–63

18. Zimmermann EA, Schaible E, Bale H et al. Age-related changes in the plasticity and toughness of human cortical bone at multiple length scales. Proc Natl Acad Sci USA 2011; 108:14416

19. Akkus O, Polyakova-Akkus A, Adar F, Schaffler M. Aging of microstructural compartments in human compact bone. J BoneMiner Res. 2003;18:1012–1019

20. Currey J. The mechanical consequences of variation in the mineral content of bone. J Biomechanics. 1969;2:1-11.

21. Zebaze RM, Ghasem-Zadeh A, Bohte A, et al. Intracortical remodelling and porosity in the distal radius and post-mortem femurs of women: a cross-sectional study. Lancet. 2010;375:1729–36.

22. Schaffler MB, Burr DB. Stiffness of compact bone: effects of porosity and density. J Biomech. 1988;21:13–6

23. Yeung SSY, Reijnierse EM, Pham VK et al J Cachexia, sarcopenia and muscle. Sarcopenia and its association with falls and fractures in older adults: A systematic review and meta-analysis. 2019; 10: 485-500.

24. Lakhani P, Prater AB, Hutson RK, et al. Machine learning in radiology: applications beyond image interpretation. J Am Coll Radiol. 2018;15:350–9

25. Pedoia V, Caliva F, Kazakia G et al Augmenting osteoporosis imaging with machine learning. Current osteoporosis reports 2021; 19: 699-709

26. King SH and Shin CS Application of machine learning in bone and mineral research. Endocrine and metab. 2021; 36:928-37

27. Kong SH, Ahn D, Kim B, Srinivasan K et al. A novel fracture prediction model using machine learning in a community-based cohort. JBMR® Plus. 4 (3), e10337

28. Sornay-Rendu E, Boutroy S, François Duboeuf F, Chapurlat RD. Bone microarchitecture assessed by HR-pQCT as predictor of fracture risk in postmenopausal women: the OFELY Study. J Bone Miner Res. 2017;32:1243–51.

29. Arlot M, Sornay-Rendu E, Garnero P, Vey-Marty B, Delmas PD. Apparent pre- and postmenopausal bone loss evaluated by DXA at different skeletal sites in women: the OFELY cohort. J Bone Miner Res. 1997;12:883–90.

30. Chapurlat R, Pialat JB, Merle B, Confavreux E, Duvert F, Fontanges E, et al. The QUALYOR (QUalite Osseuse LYon Orleans) study: a new cohort for non-invasive evaluation of bone quality in postmenopausal osteoporosis. Rationale and study design. Arch Osteoporos. Dec 27 2017;13(1):2. Epub 2017/12/29.

31. Biver E, Durosier-Izart C, van Rietbergen B et al. Evaluation of radius microstructure and areal bone mineral density improves fracture prediction in postmenopausal women. J Bone Miner Res. 2018;33:328–37.

32. Laib A, Häuselmann HJ, Rüegsegger P. In vivo high-resolution 3D-QCT of the human forearm. Technol Health Care. 1998;6: 329–37.

33. Kanis JA, Johnell O, Oden A, Johansson H, McCloskey E. FRAX and the assessment of fracture probability in men and women from the UK. Osteoporos Int. 2008;19(4):385–97.

34. Huang, G., Liu, Z., Van Der Maaten, L. and Weinberger, K.Q., 2017. Densely connected convolutional networks. In Proceedings of the IEEE conference on computer vision and pattern recognition (pp. 4700-8).

35. Kingma, D.P. and Ba, J., 2014. Adam: A method for stochastic optimization. arXiv preprint arXiv:1412.6980.

36. Paszke, A., Gross, S., Massa, F., Lerer, A., Bradbury, J., Chanan, G., Killeen, T., Lin, Z., Gimelshein, N., Antiga, L. and Desmaison, A., 2019. Pytorch: An imperative style, high-performance deep learning library. Advances in neural information processing systems, 32, pp.8026-37.

37. Selvaraju, R.R., Cogswell, M., Das, A., Vedantam, R., Parikh, D. and Batra, D., 2017. Grad-cam: Visual explanations from deep networks via gradient-based localization. In Proceedings of the IEEE international conference on computer vision (pp. 618-26).

38. Pepe, M. S. 2003. The Statistical Evaluation of Medical Tests for Classification and Prediction. Oxford: Oxford University Press.

39. Huettner, Frank; Sunder, Marco (2012): Axiomatic arguments for decomposing goodness of fit according to Shapley and Owen values. Electronic Journal of Statistics 6, 1239-50.

40. Zebaze R, Atkinson E, Peng Y, et al Increased Cortical porosity and reduced trabecular density are not necessarily synonymous with bone loss and microstructural deterioration. JBMR Plus 2019;3(4): e10078-85

41. Ghasem-Zadeh A, Bui M, Seeman E et al. Bone microarchitecture and estimated failure load are deteriorated whether patients with chronic kidney disease have normal bone mineral density, osteopenia or osteoporosis. Bone 2022; 154 116260

42. O'Brien FJ, Taylor D, Clive Lee T. The effect of bone microstructure on the initiation and growth of microcracks. J Orthop Res 2005; 23:475–80

43. Currey JD Effects of differences in mineralization on the mechanical properties of bone. Phil Trans. Royal Soc.Lond. 1984; 304:509-18.

44. Yeni YN, Brown CU, Wang Z, Norman TL. The influence of bone morphology on fracture toughness of the human femur and tibia. Bone 1997;21:453-9.

45. Yeni YN, Norman TL (2000) Calculation of porosity and osteonal cement line effects on the effective fracture toughness of cortical bone in longitudinal crack growth. J Biomed Mater Res 51:504–9

46. Burr DB, Schaffler MB, Frederickson RG (1988) Composition of the cement line and its possible mechanical role as a local interface in human compact bone. J Biomech 21:939–94.

47. Ascenzi A, Bonucci E (1967) The tensile properties of single osteons. Anat Rec 158:375–86

48. Goldman HM, Bromage TG, Thomas CD, Clement JG (2003) Preferred collagen fiber orientation in the human mid-shaft femur. Anat Rec A Discov Mol Cell Evol Biol 2003; 272:434–45

49. Buehler MJ (2008) Nanomechanics of collagen fibrils under varying cross-link densities: atomistic and continuum studies. J Mech Behav Biomed Mater 1:59–67

50. Tang SY, Vashishth D Non-enzymatic glycation alters microdamage formation in human cancellous bone. Bone 2010; 46:148–54

51. Nyman JS, Roy A, Shen X, Acuna RL, Tyler JH, Wang X The influence of water removal on the strength and toughness of cortical bone. J Biomech 2006; 39:931–8

52. Hernandez CJ, Gupta A, Keaveny TM (2006) A biomechanical analysis of the effects of resorption cavities on cancellous bone strength. J Bone Miner Res 2006; 21:1248–55

53. Fantner GE, Hassenkam T, Kindt JH Sacrificial bonds and hidden length dissipate energy as mineralized fibrils separate during bone fracture. Nat Mater 2005; 4:612–6

Table 1. Median and interquartile ranges (IQR) for Structural Fragility Score-Artificial Intelligence (SFS-AI), Fracture Risk Assessment score (FRAX) with bone mineral density (BMD) and femoral neck BMD in women remaining fracture-free and women having Any Fragility Fractures or Major Fragility Fractures during 5 years follow-up.

	Non-Fracture (N = 350)		All Fragility Fractures (54)			Major Fragility Fractures (N = 24)		
	Median	IQR	Median	IQR	p-value	Median	IQR	p-value
SFS-AI	0.45	0.10	0.51	0.08	<0.001	0.50	0.10	<0.001
FRAX with BMD	6.00	5.10	7.70	7.30	0.160	7.85	7.10	0.304
BMD	-1.64	0.88	-1.69	0.98	0.961	-1.77	0.75	0.292

p-values comparing women with and without incident fractures computed using robust regression adjusted for age and cohort.

Table 2 Performance of the Structural Fragility Score-Artificial Intelligence (SFS-AI) using data in women of any age and women aged 65 years and over

		All women of any age				Women aged 65 and older			
		Any Fragility Fracture (N = 422)		Major Fragility Fracture (N = 383)		Any Fragility Fracture (N = 236)		Major Fragility Fracture (N = 208)	
		Est	95% CI	Est	95% CI	Est	95% CI	Est	95% CI
AUC	Unadjusted	0.78	(0.73, 0.84)	0.76	(0.67, 0.85)	0.78	(0.71, 0.85)	0.76	(0.63, 0.88)
	Adjusted	0.74	(0.69, 0.79)	0.73	(0.65, 0.83)	0.73	(0.67, 0.80)	0.73	(0.61, 0.84)
OR	Unadjusted	3.44	(2.47, 4.78)	2.96	(1.85, 4.76)	3.21	(2.13, 4.83)	2.82	(1.55, 5.14)
	Adjusted	2.67	(2.03, 3.51)	2.53	(1.68, 3.82)	2.64	(1.86, 3.75)	2.54	(1.49, 4.34)
Sensitivity		65.7%	(53.4%, 76.7%)	58.1%	(39.1%, 75.5%)	74.0%	(59.7%, 85.4%)	68.2%	(45.1%, 86.1%)
Specificity		77.3%	(72.5%, 81.5%)	77.3%	(72.5%, 81.5%)	71.0%	(63.9%, 77.4%)	71.0%	(63.9%, 77.4%)

N= Sample size; Est = estimate; CI = confidence interval; Area under the curve (AUC) and odds ratios (OR) estimated with SFS-AI considered as continuous measurement and unadjusted and adjusted for age and cohort effect; Sensitivity and Specificity computed using clinical cut-off point of ≥ 0.5.

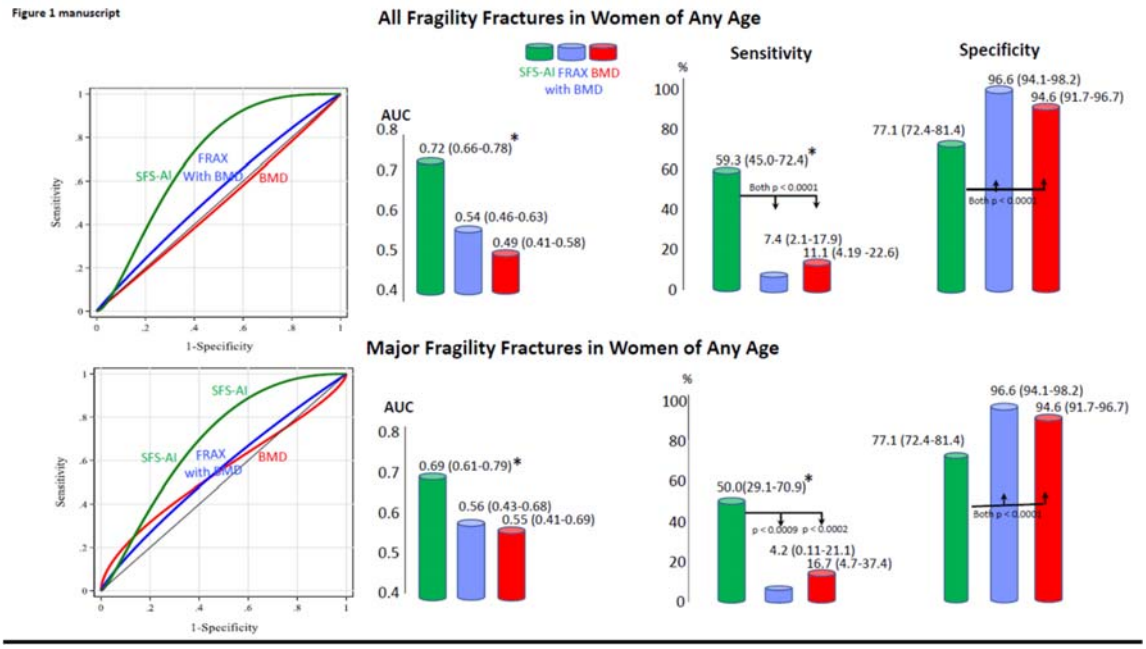

Figure 2 manuscript

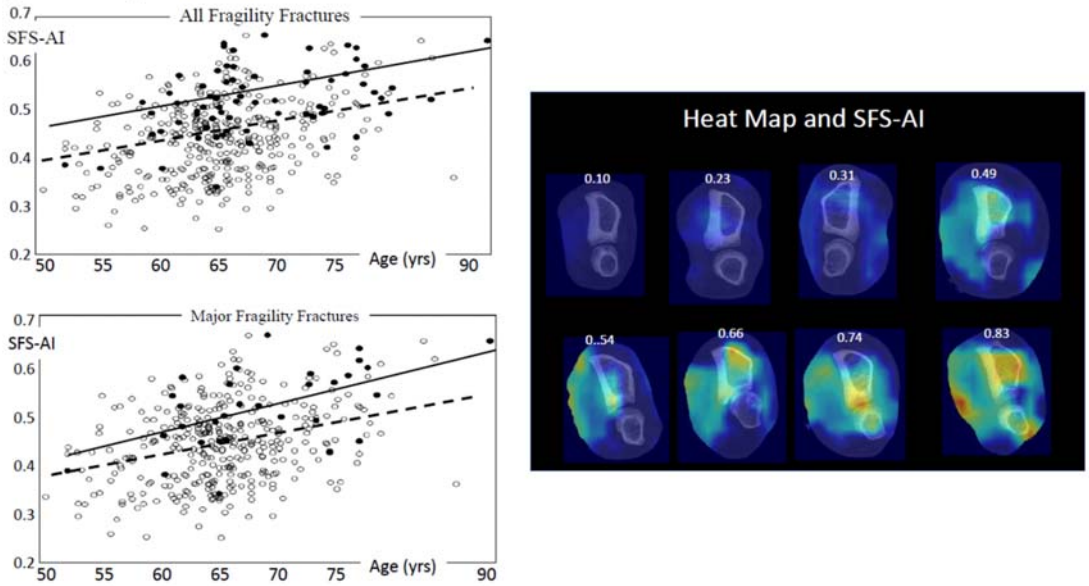

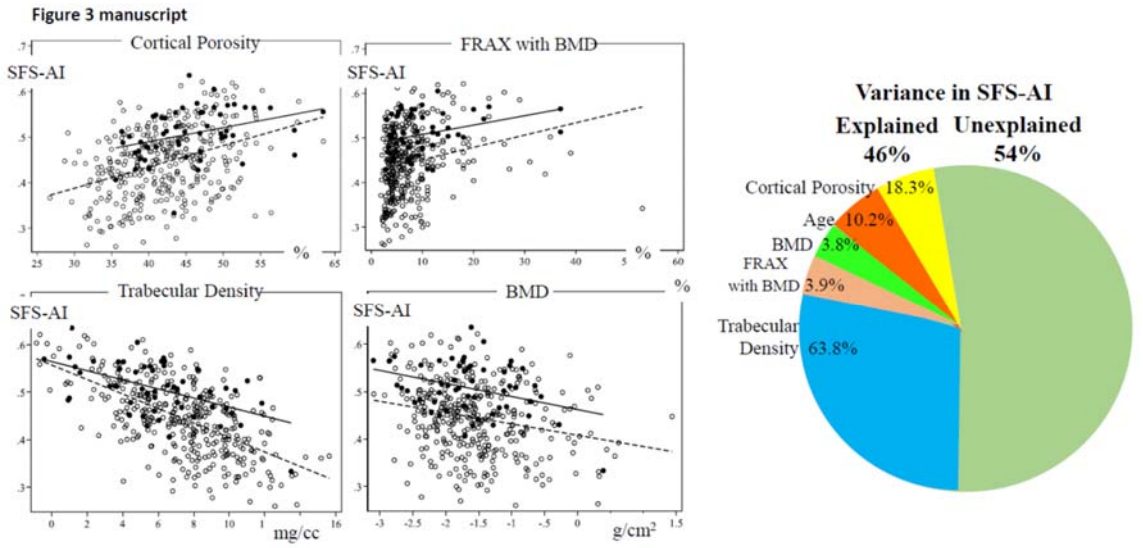

Supplementary AI methods

Deep Learning Network, training and the heat map DenseNet used dense connection between layers and achieved efficacy in feature extraction. The first layer had a 110-dimension input instead of 3-dimension input in the original DenseNet.[34] We added a transition layer using 1*1 convolution after the last denseblock of DenseNet to reduce the feature dimension from 1024 to 256 to extract a compact feature. A multi-task learning strategy was used to achieve more robust features. Extracted features were used to predict fractures during the ensuing 5-years, to predict the patient's age at the time of scanning and the duration of the fracture-free years of follow-up since scanning. The latter two tasks are included in the training to produce generalized feature representations powerful enough to be shared across different tasks.

We used a pretrained model as the initial model and 0.5 as the classification threshold for the training and validation. During training, cross-entropy loss was used as the fracture situation prediction loss, and used the mean squared error loss as the loss of age prediction and non-fracture year prediction. L1 regularization is performed on the weights of the classification layer to reduce overfitting. The model is optimized by ADAM optimizer using the four losses with weight 1 on the first three losses and weight 0.01 on the L1 regularization loss.[35] The learning rate is set as 5e-6 for the DenseNet backbone and 5e-5 for the other layers, including the transition layer and the three multi-learning branches. Pytorch is chosen to implement the model training and testing.[36] The Grad-CAM is utilized to generate the heatmap to represent the features that are extracted by the deep learning model.[37]